

Article

Scoring of Human Body-Balance Ability on Wobble Board Based on the Geometric Solution

Hang Thi Phuong Nguyen ^{1,†} , Yeongju Woo ^{1,†}, Ngoc Nguyen Huynh ¹ and Hieyong Jeong ^{1,2,*} 

¹ Department of Artificial Intelligence Convergence, Chonnam National University, 77 Yongbong-ro, Buk-gu, Gwangju 61186, Korea; 208258@jnu.ac.kr (H.T.P.N.); 218860@jnu.ac.kr (Y.W.); 217019@jnu.ac.kr (N.N.H.)

² Graduate School of Medicine, Osaka University, 1-7 Yamadaoka, Suita 565-0871, Osaka, Japan

* Correspondence: h.jeong@jnu.ac.kr; Tel.: +82-62-530-3427

† These authors contributed equally to this work.

Abstract: Many studies have reported that the human body-balance ability was essential in the early detection and self-management of chronic diseases. However, devices to measure balance, such as motion capture and force plates, are expensive and require a particular space for installation as well as specialized knowledge for analysis. Therefore, this study aimed to propose and verify a new algorithm to score the human body-balance ability on the wobble board (HBBAWB), based on a geometric solution using a cheap and portable device. Although the center of gravity (COG), the projected point of the center of mass (COM) on the fixed ground, has been used as the index for the balance ability, generally, it was not proper to use the COG under the condition of no fixed environment. The reason was that the COG index did not include the information on the slope for the wobble. Thus, this study defined the new index as the perpendicular-projection point (PPP), which was the projected point of the COM on the tilted plane. The proposed geometric solution utilized the relationship among three points, the PPP, the COM, and the middle point between the two feet, via linear regression. The experimental results found that the geometric solution, which utilized the relationship between the three angles of the equivalent model, enabled us to score the HBBAWB.

Keywords: center of gravity; center of mass; human balance ability on wobble board; perpendicular-projection point; kinematics; geometric solution



Citation: Nguyen, H.T.P.; Woo, Y.; Huynh, N.N.; Jeong, H. Scoring of Human Body-Balance Ability on Wobble Board Based on the Geometric Solution. *Appl. Sci.* **2022**, *12*, 5967. <https://doi.org/10.3390/app12125967>

Academic Editors: Richie Gill, Alberto Leardini and Tung-Wu Lu

Received: 27 April 2022

Accepted: 8 June 2022

Published: 11 June 2022

Publisher's Note: MDPI stays neutral with regard to jurisdictional claims in published maps and institutional affiliations.



Copyright: © 2022 by the authors. Licensee MDPI, Basel, Switzerland. This article is an open access article distributed under the terms and conditions of the Creative Commons Attribution (CC BY) license (<https://creativecommons.org/licenses/by/4.0/>).

1. Introduction

Balance is essential to remain steady when walking, sitting up, standing, or playing sports. People utilize balance constantly in their daily routines, without even thinking about it. There is evidence that balance training produces moderate-to-large reductions in the risk of body imbalance, fall, or subsequent injuries, and contributes to the optimization of motor performance [1–3]. Various factors lead to decreased balance control, such as sensory feedback, muscle strength, cognitive function, and biomechanical constraints [4]. For example, our previous study, related to gait analysis for older adults, found that the symmetry between left and right feet differed in fast-walking speed because elderly patients with diabetes had a worse balance than healthy elderly adults [5,6]. Therefore, balance training is practical for adults and is suitable for people of any age. Furthermore, in some studies, balance-ability training is used to improve postural control in many sports (and for many fitness levels), such as basketball, baseball, soccer, etc. [7–9]. Thus, people need to train and evaluate their balance ability to enhance their capacity and prevent falls, especially older patients. The authors have proposed a non-invasive and low-cost system for trainees who would like to improve their balance ability and have been studying methods to help improve health and quality of life by self-health management [10].

Home-training apps based on artificial intelligence (AI) are an effective solution to help users exercise with the correct posture, even if users exercise alone at home [11,12].

Representative developed apps include Aaptiv Coach, Fitbod, VI Trainer, Kaia Personal Trainer, VAY Fitness Coach, Millie Fit, infiGro, and Gymfitty [13]. These apps can automatically calculate exercise frequency by estimating exercise posture with extracted key points through AI-based human-pose-estimation technology. Most people are getting busier, so they have no time to exercise regularly. Maintaining regular exercise is even more challenging. Thus, these kinds of apps are helpful. The primary role of a human coach is to manage the trainee to ensure they continue to exercise at first. Then, the other significant role of a coach is to evaluate the trainee's exercises with the correct pose. Unfortunately, these developed apps do not provide the function of the second important role, which is assessing the posture of the trainee [14,15].

Examples of exercise-posture-evaluation systems include expensive motion-capture and force-plate systems [16,17]. The marker-based motion-capture system is a system that attaches a marker to the subject's body, recognizes the attached marker by a plurality of cameras, reconstructs the subject's motion in a computer, and evaluates the posture of the body in various situations. It seems complicated to proceed from experimental preparation to analysis alone at home. Markerless motion capture uses standard video and often relies on deep-learning-based software (pose-estimation algorithms) to perform movement analysis with reduced data collection and processing time, compared to marker-based methods [18]. However, the hardware employs either depth cameras or standard video cameras and may be used in single- or multi-camera systems, and it is more expensive than an RGB camera. Although with the force-plate system is not necessary to attach the marker to the human body, this system needs professional knowledge to understand the analysis results of the center of pressure (COP) and the vertical-reaction forces (VRFs) during standing, after removing the visual information [19–22]. Therefore, there is a need for a low-cost device and an evaluating method that anyone can easily understand. Thus, the current study aimed to propose and verify a new algorithm to score the human body-balance ability on the wobble board (HBBAWB), based on a geometric solution using a cheap and portable device.

The contribution of this study was mainly three points: the first point was to replace the human body on the wobble with an equivalent model; the second was to define a new index to score the balance ability, instead of the generally used center of gravity (COG); the final was to digitize the HBBAWB.

2. Experimental Conditions

2.1. Human Participants

The human participants included nine students and one researcher (four females and six males; 28.8 ± 6.9 years old; 66.1 ± 11.9 kg; 167.1 ± 8.34 cm) from the university. No human participants from either group reported a significant back or lower-limb pathological condition, medication use, or a history of neurological disease that might influence standing balance. In addition, no significant difference in the body mass index (BMI) was observed in the BMI of all the human participants (23.6 ± 3.9 kg/m²).

The experimental procedures were performed under the Declaration of Helsinki and approved by the Ethics Committee of the Clinical Trial Center, Department of Medical Innovation, Osaka University Hospital. Furthermore, all the human participants submitted their consent before the experiment (no. 305, 21 August 2014).

2.2. Experimental Environment and System

Figure 1a shows an overview of the experimental environment and system. A and B represent the locations of the two feet. The experimental system consists of a single RGB camera, a C270 HD webcam, and a wobble board. The role of the RGB camera is to detect AI-based key points via acquired images. The maximum resolution supported by the camera is width \times height = 1280×720 at 30 frames per second (fps). The resolution can change, and the default resolution supported by OpenCV (640×480) was used in this experiment. The specification of the camera is height \times width \times depth = 72.91 mm \times

31.91 mm × 66.64 mm, and the bodyweight of the camera is 75 g. The size of the wobble balance board is width × depth × height = 480 mm × 290 mm × 80 mm. The material is EVA + wood + Velcro. So, the board has a little elasticity, but it is possible to use this with a body weight below 100 kg.

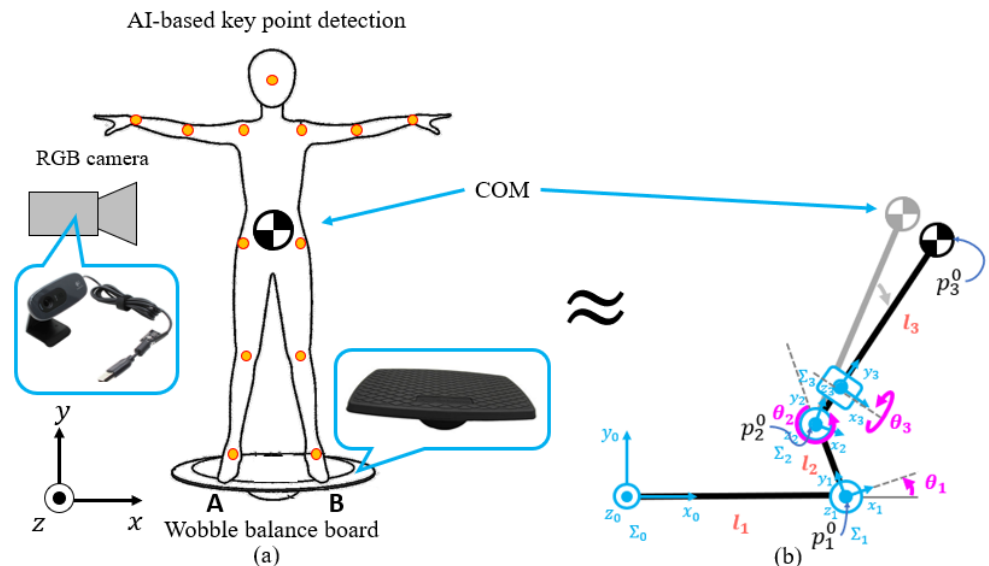


Figure 1. (a) An overview of experimental environment, system, and (b) a definition of variables for an equivalent model, which is expressed as an inverted pendulum on wobble board.

This study applies the MediaPipe Pose, which is an estimation algorithm from MediaPipe (version 0.8.9) for extracting joints [23]. MediaPipe Pose is a machine-learning (ML) solution for high-fidelity body-pose tracking. MediaPipe infers the number of 33 three-dimensional landmarks and background-segmentation masks on the whole body from RGB video frames, while utilizing the BlazePose research powers of the ML Kit Pose Detection API. Current state-of-the-art approaches rely primarily on powerful desktop environments for inference. On the contrary, this method achieves real-time performance on most modern mobile phones and desktops/laptops, using Python, and even via the web [23].

A USB cable was used to connect the RGB camera to the computer. This study applied the MediaPipe Pose in extracting the joints of human subjects standing on the wobble board and in front of the camera. Participants stood barefoot, shoulder-width apart, and in the middle of the wobble balance board, staring straight ahead, looking at a camera, and standing as still as possible for 20 s (trial duration). During the experiment time, the tilted angle of the wobble and human movement were calculated and collected. Jupyter Notebook, as one kind of Python text editor, was used for Python programming. The Python version was 3.7, and the MediaPipe package version was 0.8.9.

3. Equivalent Model

3.1. Estimation of Center of Mass

The center of mass (COM) is the critical position at which the weighted position vectors of all the system parts sum up to zero. The COM is a position defined relative to an object or system of things. It is the average position of all the system parts, weighted according to body masses. Calculating the appropriate weight for each body segment leads to the COM estimation improving more accurately [24,25]. All 33 key points based on human-pose estimation are divided into eight parts: head, trunk, shoulder, arm, hand, thigh, calf, and foot. A MediaPipe Pose solution was applied to the input images to extract 33 key points, representing an individual's joints on the three-dimensional image.

Figure 2 shows an example of the detected key points as a variable in a segmented part (arm), in order to explain how to calculate the location of the COM. The COM of this

part can be determined from the proximal-end and distal-end coordinates and the segment-length percentage. The specific coordinates of the COM of one part can be calculated as follows [26]:

$$\begin{aligned} X_{CM} &= X_D(\%cm) + X_P(1 - \%cm), \\ Y_{CM} &= Y_D(\%cm) + Y_P(1 - \%cm), \\ Z_{CM} &= Z_D(\%cm) + Z_P(1 - \%cm), \end{aligned} \tag{1}$$

where X_{CM}, Y_{CM}, Z_{CM} represent the coordinate of the COM, (X_D, Y_D, Z_D) are the coordinate of the distal end of the segment, X_P, Y_P, Z_P are the coordinate of the proximal end, and $\%cm$ is the COM position ratio divided by 100, respectively. The COM calculation of the human body has also applied the equation individually to each axis [26]:

$$\begin{aligned} X_{COM} &= \frac{\sum_{i=0}^n m_i x_i}{M}, \\ Y_{COM} &= \frac{\sum_{i=0}^n m_i y_i}{M}, \\ Z_{COM} &= \frac{\sum_{i=0}^n m_i z_i}{M}, \end{aligned} \tag{2}$$

where $X_{COM}, Y_{COM}, Z_{COM}$ is the coordinate of the COM along the x, y, and z-axis, M is the total mass of the human body, n is the number of body parts, m_i is the mass of the i-th part, and x_i is the coordinate from the x-axis of i-th portion, respectively.

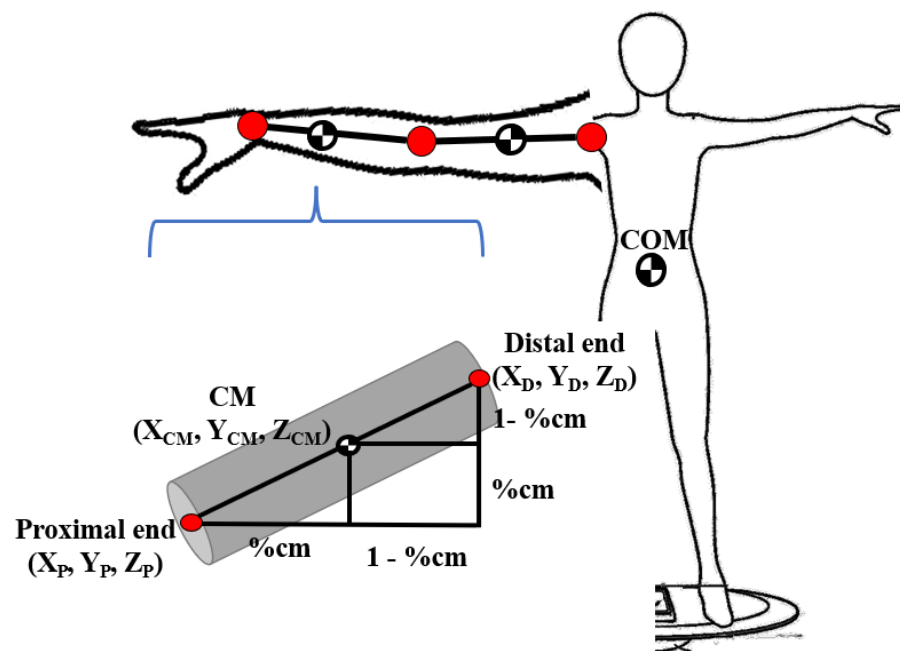


Figure 2. An example of detected key points as variables in a segmented part (arm), in order to explain how to calculate the location of the center of mass (COM).

3.2. Forward Kinematics

Figure 1b represents a definition of variables for an equivalent model, which is expressed as an inverted pendulum on a wobble board. Σ_0 represents the world coordinate, Σ_1 represents that for the contact point between the wobble and the ground, and Σ_2 and Σ_3 represent that for the surface of the wobble, respectively. p_1^0 indicates the location of Σ_1 at the Cartesian coordinate system in terms of Σ_0 , p_2^0 indicates that of Σ_2 and Σ_3 in terms of Σ_0 , and p_3^0 indicates that of the COM, respectively. The inverted pendulum is the pendulum that has its COM above its pivot point. It is unstable and will fall over without additional support. The inverted pendulum can be used as an equivalent model, when the COM of the pendulum is regarded as the COM of the human body [27].

Consider the inverted pendulum with torque actuation at two joints, θ_2 and θ_3 , and there is no torque actuation at the joint of θ_1 for the wobble board. Namely, θ_1 is the free joint. The rotation of θ_1 and θ_2 is the mediolateral (ML) axis and that of θ_3 is the anteroposterior (AP) axis, as shown in Figure 1b. l_1 represents the distance from the world coordinate of Σ_0 to the board coordinate of Σ_1 , which is in contact with the ground. l_2 represents the height of the wobble board, and l_3 represents that from the plane of the wobble board to the COM. The location of p_1^0, p_2^0 , and p_3^0 can be calculated by $q = [\theta_1, \theta_2, \theta_3]^T$ and all link lengths of l_1, l_2 , and l_3 [28]:

$$\begin{aligned}
 p_1^0 &= T_1^0 [0; 0; 0; 1]^T \\
 &= \begin{bmatrix} c_1 & -s_1 & 0 & l_1 \\ s_1 & c_1 & 0 & 0 \\ 0 & 0 & 1 & 0 \\ 0 & 0 & 0 & 1 \end{bmatrix} \begin{bmatrix} 0 \\ 0 \\ 0 \\ 1 \end{bmatrix} = \begin{bmatrix} l_1 \\ 0 \\ 0 \\ 1 \end{bmatrix}, \\
 p_2^0 &= T_1^0 T_2^1 [0; 0; 0; 1]^T \\
 &= \begin{bmatrix} c_1 & -s_1 & 0 & l_1 \\ s_1 & c_1 & 0 & 0 \\ 0 & 0 & 1 & 0 \\ 0 & 0 & 0 & 1 \end{bmatrix} \begin{bmatrix} c_2 & -s_2 & 0 & 0 \\ s_2 & c_2 & 0 & l_2 \\ 0 & 0 & 1 & 0 \\ 0 & 0 & 0 & 1 \end{bmatrix} \begin{bmatrix} 0 \\ 0 \\ 0 \\ 1 \end{bmatrix} = \begin{bmatrix} l_1 - l_2 s_1 \\ l_2 c_1 \\ 0 \\ 1 \end{bmatrix}, \\
 p_3^0 &= T_1^0 T_2^1 T_3^2 [0; 0; 0; 1]^T
 \end{aligned} \tag{3}$$

$$\begin{aligned}
 &= \begin{bmatrix} c_1 & -s_1 & 0 & l_1 \\ s_1 & c_1 & 0 & 0 \\ 0 & 0 & 1 & 0 \\ 0 & 0 & 0 & 1 \end{bmatrix} \begin{bmatrix} c_2 & -s_2 & 0 & 0 \\ s_2 & c_2 & 0 & l_2 \\ 0 & 0 & 1 & 0 \\ 0 & 0 & 0 & 1 \end{bmatrix} \begin{bmatrix} 1 & 0 & 0 & 0 \\ 0 & 1 & 0 & l_3 \\ 0 & 0 & 1 & 0 \\ 0 & 0 & 0 & 1 \end{bmatrix} \begin{bmatrix} 0 \\ 0 \\ 0 \\ 1 \end{bmatrix} = \begin{bmatrix} l_1 - l_3 s_{12} - l_2 s_1 \\ l_3 c_{12} + l_2 c_1 \\ 0 \\ 1 \end{bmatrix},
 \end{aligned}$$

$$\begin{aligned}
 p_3^0 &= R_3^2 p_3^0 \\
 &= \begin{bmatrix} 1 & 0 & 0 & 0 \\ 0 & c_3 & -s_3 & 0 \\ 0 & s_3 & c_3 & 0 \\ 0 & 0 & 0 & 1 \end{bmatrix} \begin{bmatrix} l_1 - l_3 s_{12} - l_2 s_1 \\ l_3 c_{12} + l_2 c_2 \\ 0 \\ 1 \end{bmatrix} = \begin{bmatrix} l_1 - l_3 s_{12} - l_2 s_1 \\ c_3 (l_3 c_{12} + l_2 c_1) \\ s_3 (l_3 c_{12} + l_2 c_1) \\ 1 \end{bmatrix},
 \end{aligned}$$

where T_1^{i-1} for $i \geq 0$ gives the relationship between the body frame of Σ_i and the body frame of Σ_{i-1} , s_j and c_j for $j > 0$ are shorthand for $\sin \theta_j$ and $\cos \theta_j$, and $s_{(j)(j+1)}$ and $c_{(j)(j+1)}$ are shorthand for $\sin(\theta_j + \theta_{j+1})$ and $\cos(\theta_j + \theta_{j+1})$. Now, the location of p_3^0 can be described by the relationship between three angles and links.

4. Methods

4.1. Definition of Perpendicular-Projection Point

Before explaining the proposed algorithm, it is necessary to define some parameters, including a new one. Figure 3 shows an illustration of the human body on the wobble board with the necessary parameters: the perpendicular-projection point (PPP), the base of the foot (BOF), the center of gravity (COG), the line of gravity, and the perpendicular line under the stable (left side) and unstable (right side) balance conditions. Remarkably, the new parameter of the PPP in this study indicates the projection point from the COM to the plane on the wobble board, expressed as the yellow-colored point on the plane. The BOF represents the middle point between the two feet, and the COG represents the projection point from the COM to the fixed ground, which is expressed as the red-colored point on the wobble board.

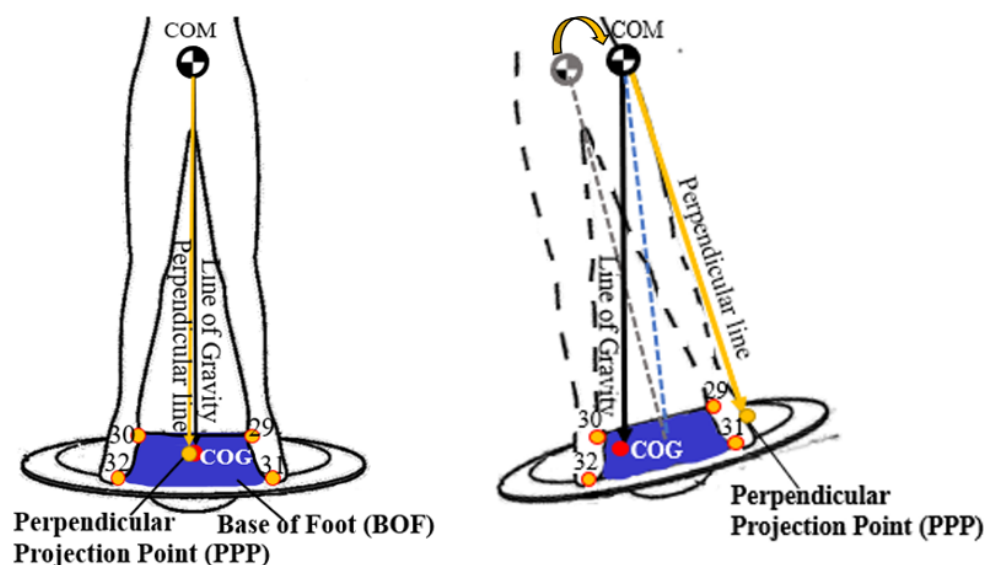


Figure 3. An illustration of the human body on the wobble board with necessary parameters: perpendicular-projection point (PPP), the base of foot (BOF), the center of gravity (COG), the line of gravity, and the perpendicular line under the stable (**left side**) and unstable (**right side**) balance conditions.

When the plane of the wobble is not tilted in any direction, the COG is equal to the PPP, as shown in Figure 3 (left side). However, the COG becomes different from the PPP when the plane is tilted toward the ML plane. For example, Figure 3 (right side) shows that the PPP moves to the opposite side (left side) when the wobble is tilted to the right side in the ML plane. Without any fixed-body support systems, if the balance board tilts, the body will tend to lean in the opposite direction of the balance-board tilt, to offset the torque due to gravity [4].

It could be said that the location of the PPP is directly related to the tilt angle of θ_1 for the wobble board, as shown in Figure 1b. Thus, the index based on the location of the PPP plays an essential role in scoring the HBBAWB.

4.2. Boundary Conditions

Figure 4 shows a description of the boundary condition, based on the location of the PPP and the state of human balance on the wobble board under the boundary condition. The user stands on the plane of the wobble board, then tries to keep the stable balance condition. Here, all points of kp_{29} , kp_{30} , kp_{31} , and kp_{32} represent key points for two feet, which can be seen from the pose landmark model in the MediaPipe Pose at the upper side. Two points, mp_{29-31} and mp_{30-32} , represent each middle point between two key points of each foot. In this study, mp_{29-31} and mp_{30-32} were regarded as the boundary condition, worthy of scoring the HBBAWB.

When the location of the PPP for the user becomes out of the boundary condition, a zero score is the unstable balance condition. Thus, there is no need to score the HBBAWB because the wobble board contacts the ground in this case, as shown in Figure 4 (right side). When the PPP coincided with the BOF, a 100 score is a stable condition. Thus, it is possible to draw the gray-colored circle as the allowable boundary range with the radius of the distance between the BOF and the mp_{29-31} or mp_{30-32} . For the direction discrimination, such as left and right, the right side indicates positive, and the left indicates negative.

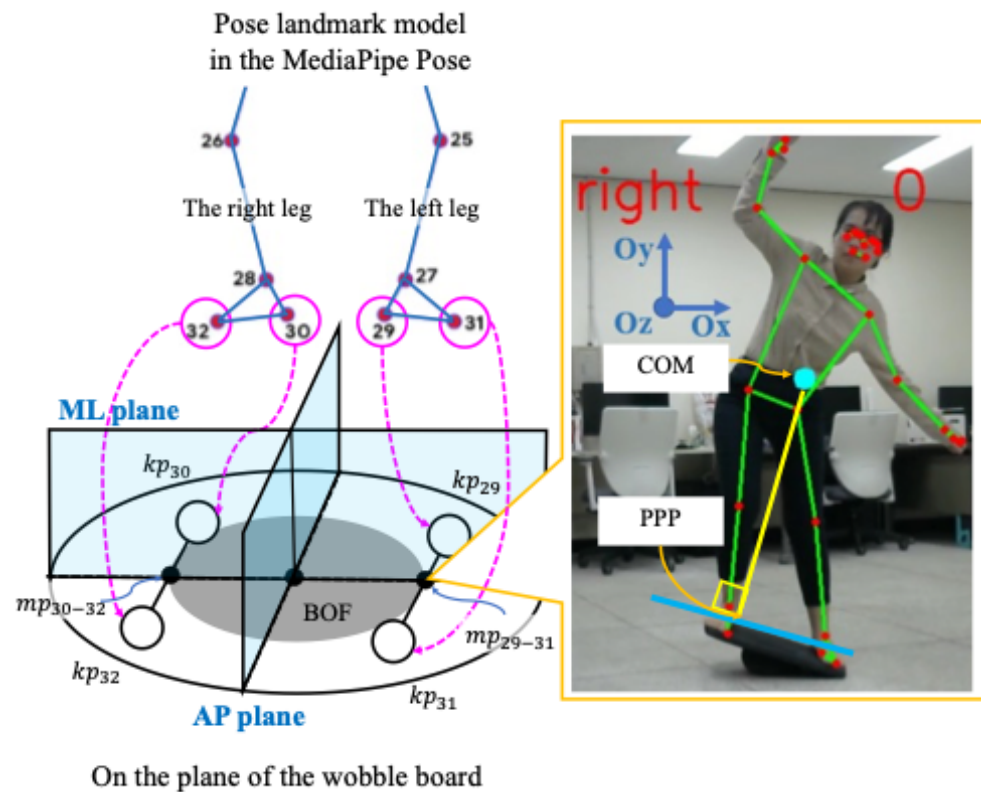


Figure 4. A description of boundary conditions based on the location of the perpendicular-projection point (PPP), and the state of human balance on the wobble board under the boundary condition.

4.3. Scoring Algorithm

Figure 5 shows an explanation for the proposed algorithm to score the HBBAWB, based on the geometric solution within the boundary condition. For example, when the projected location for the three points of the PPP, BOF, and COG is equal, the score is 100 points. In this case, we can get the \min_{α} (=zero), which means the minimum of the angle of α . When the location of the PPP is on the boundary line of the gray-colored circle, the score becomes zero. In this case, we can get the \max_{α} , which means the maximum of the angle of α in the triangle. Thus, the angle α can be decided within the range of $\min_{\alpha} \leq \alpha \leq \max_{\alpha}$ within the boundary condition.

Since α can be expressed as the one angle in the triangle made by the three PPP, BOF, and COM points, it is possible to calculate the score as follows,

$$Score = \left(1 - \frac{\alpha}{\max_{\alpha}}\right) \times 100. \tag{4}$$

As a result, it is confirmed that the dependent vector of the score becomes the linear regression with the independent vector of the angle of α .

The angle of α is calculated by the geometric solution, to find the angle between the three given key points extracted by the MediaPipe solution. Figure 6 shows an example of calculating the angle between the three points in three dimensions. The angle between the three given points $A(x_A, y_A, z_A)$, $B(x_B, y_B, z_B)$, $C(x_C, y_C, z_C)$ is β , and the angle of β is determined by the mathematical formula of the angle between two vectors, \vec{BA} and \vec{BC} :

$$\beta = \cos^{-1} \frac{(x_A - x_B)(x_C - x_B) + (y_A - y_B)(y_C - y_B) + (z_A - z_B)(z_C - z_B)}{\sqrt{(x_A - x_B)^2 + (y_A - y_B)^2 + (z_A - z_B)^2} \sqrt{(x_C - x_B)^2 + (y_C - y_B)^2 + (z_C - z_B)^2}} \tag{5}$$

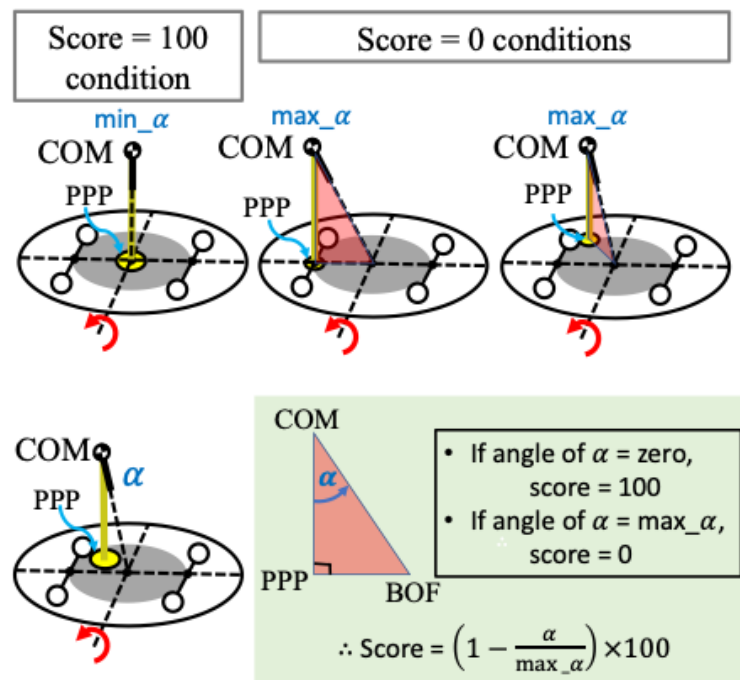


Figure 5. An explanation for the proposed algorithm to score the human body-balance ability on the wobble board (HBBAWB) through the geometric solution under the boundary condition.

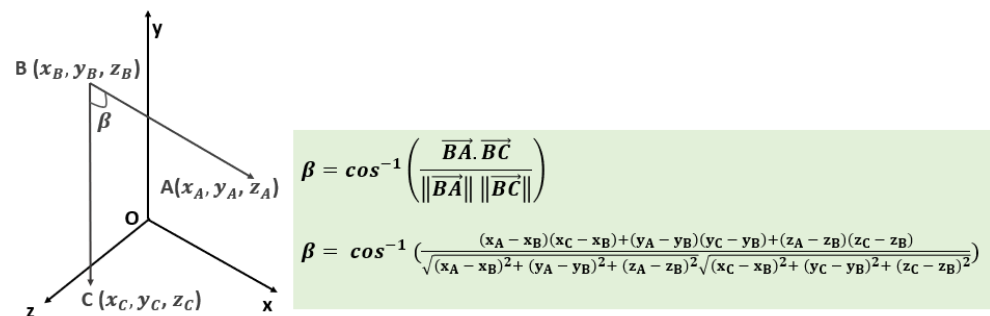


Figure 6. The example of calculating the angle between three points (A, B, C) in three dimensions.

5. Results

5.1. Results of User-Interface System

Figure 7 shows the results of the UI design for the scoring system. When the user is standing on the wobble balance board, the UI system starts to calculate the score based on Equation (4). The blue-green-colored circle on the human represents the estimated COM through Equation (2), and the yellow-colored circle on the plane of the wobble represents the PPP. The upper-right side shows the current balance score, based on the geometric solution. The upper-left-side part is to instruct the user to move in a particular direction to improve the stable balance condition, while recognizing the location of the PPP. For example, when the PPP is out of the boundary condition in the right-foot direction, the user should move the COM to the right side. So, the user can find the instruction of “move right” in this part. The balance score is 96.20, which means the perpendicular line nearly coincides with the line of gravity.

As a result, the user can directly understand the current balance condition and then can see the instruction on improving the balance condition when the PPP is out of the boundary condition, using the designed UI system.

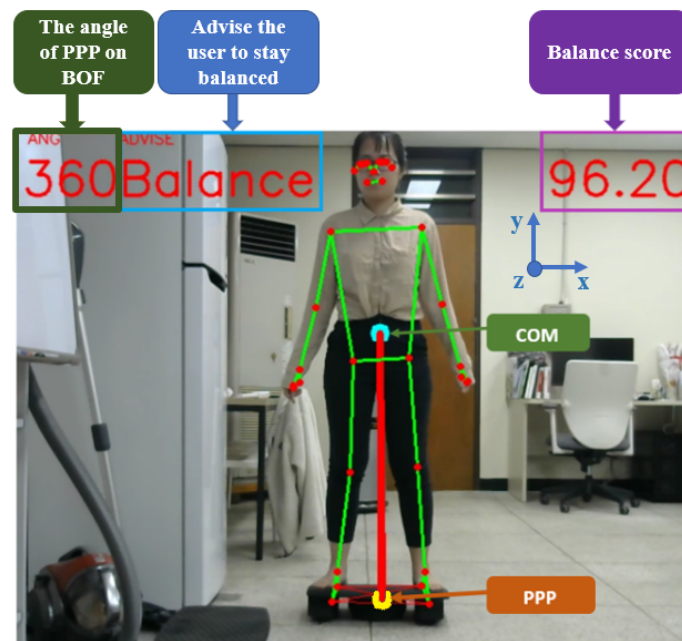
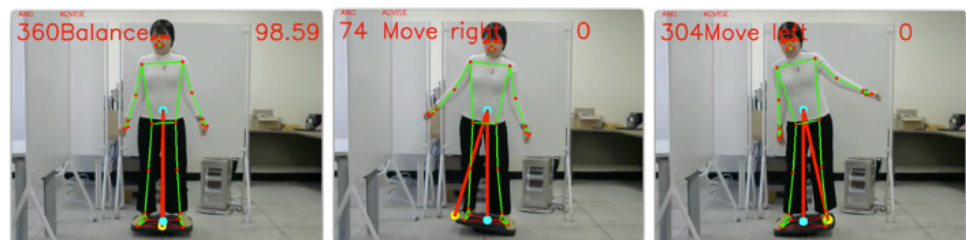


Figure 7. The results of the specifications were displayed on the screen of the scoring system.

5.2. Results of Verification of Scoring Algorithm

Figure 8 shows the results of some examples to score the HBBAWB based on the geometric solution. The blue-green colored circle on the human body indicates the location of the COM, the same colored circle on the plane shows that of COG, and the yellow-colored circle demonstrates that of the PPP.



(a) The results of the score under the boundary condition.



(b) The results of the score within the boundary condition.

Figure 8. The results of some examples to score the human body-balance ability on the wobble board (HBBAWB) based on the geometric solution: (a) represents the results under the boundary condition and (b) represents within the boundary condition.

For the results of the score under the boundary condition in Figure 8a, the score became 100 points when the PPP was equal to the COG. On the other hand, the score was zero when the PPP was on the boundary condition, regardless of being on the left or right side on the ML plane. Furthermore, the proposed algorithm enabled the user to be instructed on how to improve the current balance condition, such as “move left” and “move right”, as shown in Figure 8a. For the results of the score within the boundary condition in Figure 8b, the experimental results verified that the proposed scoring algorithm worked

well. Notably, the visualization for the location of the PPP helped the user keep a stable balance condition.

Table 1 shows the results of boundary conditions for 10 participants. In this study, \max_{α} is a variable, not a constant. Because the location of COM affected the value of \max_{α} as shown in Figure 5.

Table 1. The results of boundary conditions for ten participants.

ID	Age	Gender	Weight [kg]	Height [cm]	Max $_{\alpha}$ (°)
1	25	Female	60	155	10.47 ± 0.42
2	28	Female	57	156	10.35 ± 0.32
3	23	Female	50	162	8.40 ± 0.26
4	25	Female	52	162	8.40 ± 0.33
5	36	Male	80	170	8.77 ± 0.68
6	45	Male	80	170	9.3 ± 0.54
7	27	Male	81	170	9.70 ± 0.74
8	30	Male	69	173	9.28 ± 0.59
9	27	Male	73	176	8.32 ± 0.82
10	22	Male	59	180	8.06 ± 0.33

The different boundary conditions of \max_{α} came from the different physical conditions of each participant.

Figure 9 shows the results of the line plot between the angles of α and θ_1 . α of the blue-colored plot represents the angle between the three points of the BOF, COM, and PPP, as shown in Figure 5, and θ_1 of the orange-colored plot represents the tilted slope of the wobble board, as shown in Figure 1b. If the θ_1 value increases and the α value falls, they have an opposite direction, and the user is in a stable condition. Furthermore, the more change there is of the θ_1 value and the α value, offset under the balance condition, the better the user maintains equilibrium. Conversely, when the θ_1 line and α line go up or down together, meaning the α value and θ_1 value increase or decrease together, the user is in an unstable condition.

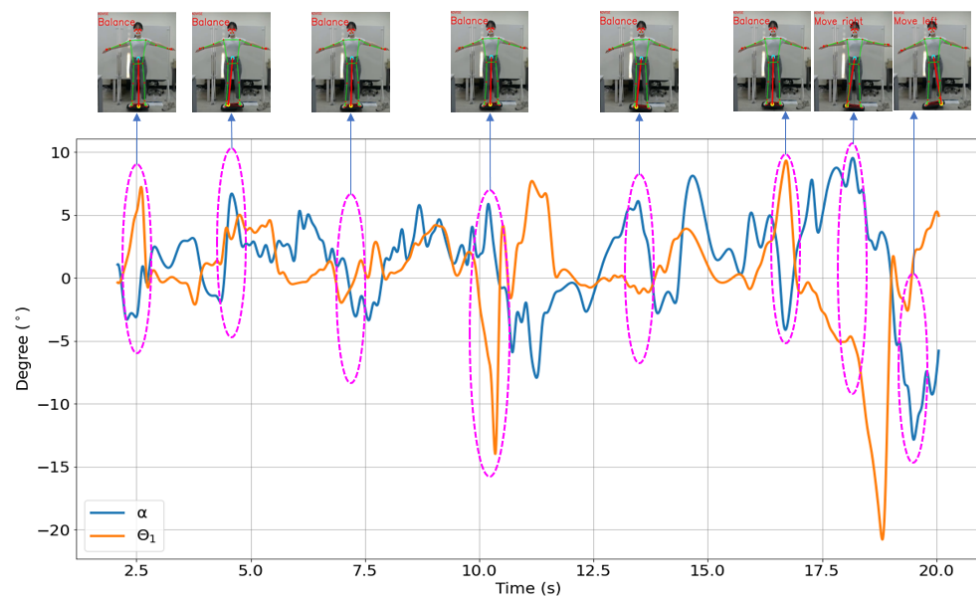


Figure 9. The results of line plot between angles of α and θ_1 : α of blue-colored plot represents the angle between three points of the base of the foot (BOF), the center of mass (COM), and the perpendicular-projection point (PPP), while θ_1 of orange-colored plot represents the tilted slope of the wobble board.

That meant that the PPP of the proposed index played an essential role in explaining the reason and cause, compared with the trajectories of the COG.

As a result, the proposed scoring algorithm enabled us to be able to score the HBBAWB, compared with a conventional method, such as the trajectories of the COG.

6. Discussion

6.1. Limitation of the Center of Gravity to Estimate Human Balance on the Wobble Board

The COM lies approximately anterior to the second sacral vertebra in the anatomical position. However, since human beings do not remain fixed in the anatomical position, the precise placement of the COM changes, relatively according to body movement. Furthermore, the vertical projection of the COM on the ground is often called the COG [29,30]. For example, the COG represents the projected point on the x - z plane, as shown in Figure 10. Although the trajectory of the COG is suitable for assessing the human-balance ability in general, it seems it is not proper that trajectories of the COG explain the HBBAWB. Furthermore, since the COG does not include information about the tilt of the wobble board, it is not easy to explain the reason and cause through these results.

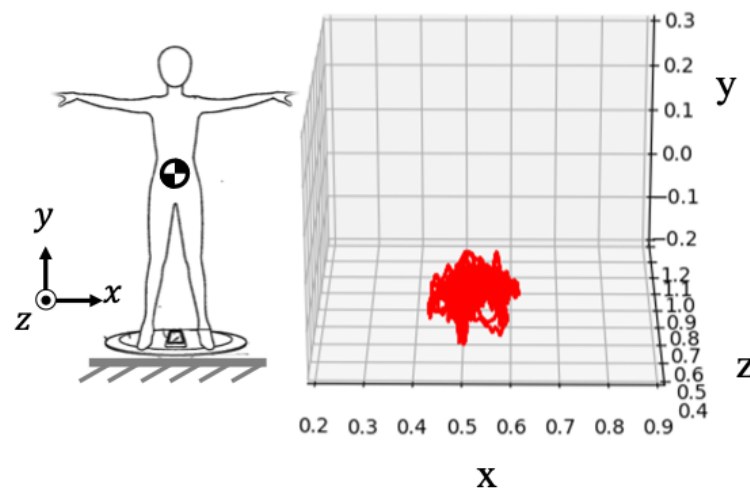


Figure 10. The results of trajectories of the center of gravity (COG) when the human subject stands on the wobble board.

6.2. Pros and Cons of Libraries and Models for Human-Pose Estimation

HPE detects human figures in images or videos. Usually, it is the identifying and classifying of the human-joint coordinates and the reconstruction of a human-skeletal representation. In the last few years, two-dimensional pose estimation approached a detection rate above 90% on all different human joints [31]. Recently, due to the success of convolutional neural networks (CNN) and accessible massive datasets, this progress has been possible [32,33]. However, these new architectures have only recently been deployed to resolve the same problem in three dimensions. Furthermore, these new three-dimensional markerless pose-estimation methods challenge competition against classical techniques and marker-based motion-capture systems. The final result requires a complete and accurate three-dimensional reconstruction of an individual's motion, from simple images with tolerance to severe occlusion [34]. Table 2 is a brief discussion of five kinds of available libraries [14].

Overall, the area can be subdivided into two- and three-dimensional pose estimations. While the accuracy can be acceptable in two-dimensional pose estimation, three-dimensional pose estimation still requires more accurate models, mainly for inference from a single image and without depth information. Therefore, some methods are pointed at the person using multiple cameras or the signals from depth sensors to achieve better predictions.

Table 2. The Pros and cons of five kinds of human-pose-estimation (HPE) libraries and models.

Methods	Pros	Cons
OpenCV [35]	<ul style="list-style-type: none"> – many tutorials to instruct the setting up and employing the models – useful built-in tools for processing and analyzing the content of images' computer-vision tasks 	<ul style="list-style-type: none"> – difficult to customize – the real-time performance is most likely poor
OpenPose [36]	<ul style="list-style-type: none"> – combined full-body keypoints detection – provide the flexibility of choosing source images from camera fields, webcams, and others 	<ul style="list-style-type: none"> – only non-commercial use – real-time performance is poor if only on the CPU
PoseNet [37]	<ul style="list-style-type: none"> – runs on lightweight devices such as a browser or mobile device – be able to estimate a single pose or multiple poses – inference time is fast 	<ul style="list-style-type: none"> – medium accuracy – be deficient for some of the pose estimation applications
Detectron2 [38]	<ul style="list-style-type: none"> – a huge amount of models available – high accuracy 	<ul style="list-style-type: none"> – no real-time performance, mostly on the CPU
AlphaPose [39]	<ul style="list-style-type: none"> – can detect both single- and multi-person poses in images or videos – pose tracking – high accuracy 	<ul style="list-style-type: none"> – only non-commercial use – mostly does not perform in real time on CPU

The difficulty of the three-dimensional pose-estimation issues is the lack of large annotated datasets with people in open environments. For example, a massive dataset for three-dimensional pose estimation, “Human3.6M”, was captured indoors. There is a continuous effort to produce new datasets that would include various data in terms of environment, clothing variety, strong articulations, etc.

6.3. The Advantages and Disadvantages of Our Method

Our results for scoring the human body-balance ability on the wobble board, based on the geometric solution, are different according to the chosen pose-estimation algorithms, which extracted the key points of the body.

We compared the results with two of the most popular HPE models, VideoPose3D and BlazePose GHUM. Figure 11 shows the results of VideoPose3D and BlazePose GHUM for the comparison of three-dimensional human-pose-estimation performance and accuracy. Seventeen double-colored circles represent the results of VideoPose3D, and seventeen red-colored circles represent the results of BlazePose GHUM in white-colored circles. The test was performed under the condition of the same hardware using a 5 s video with 640×480 dimensions and 30 frames per second (FPS). Two HPE models used 20 min for video processing with a good accuracy result.

Table 3 shows the results of the pose-estimation quality of the BlazePose GHUM model used in MediaPipe Pose. The result was evaluated through three different validation datasets: Yoga, Dance, and HIIT. The results confirmed that the used model in this study showed high performance with high accuracy. Furthermore, the human pose to keep the balance on the wobble board was similar to the Yoga pose. Thus, there was no severe problem in extracting the key points based on the BlazePose GHUM model.

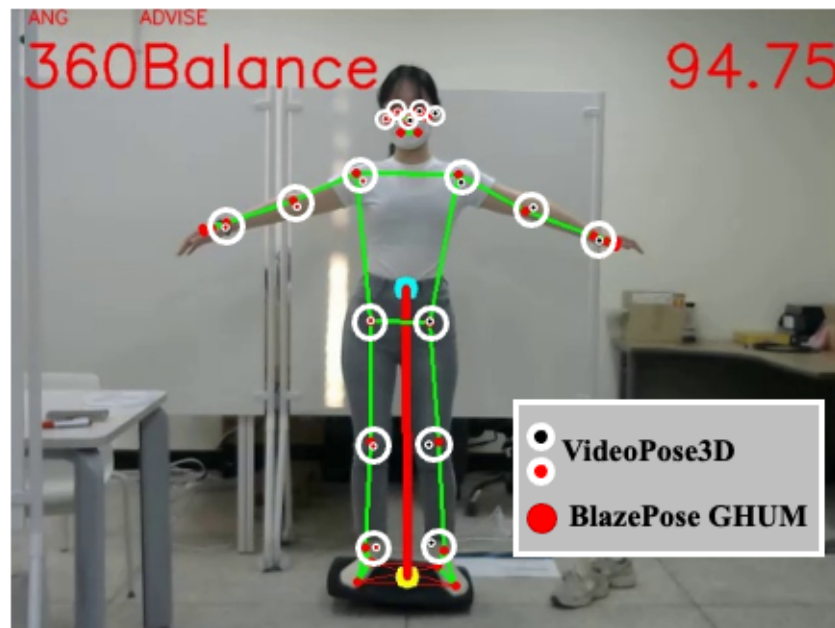


Figure 11. The results of VideoPose3D and BlazePose GHUM for the comparison of three-dimensional pose estimation performance and accuracy: seventeen double-colored circles represent the results of VideoPose3D, and seventeen red-colored circles represent that of BlazePose GHUM in white-colored circles.

Table 3. The results of pose-estimation quality of BlazePose GHUM [40,41] model in MediaPipe Pose [23].

Method	Yoga	Dance	HIIT
BlazePose GHUM (Heavy)	96.4	97.2	97.5
BlazePose GHUM (Full)	95.5	96.3	95.7
BlazePose GHUM (Lite)	90.2	92.5	93.5
AlphaPose ResNet50	96.0	95.5	96.0
Apple Vision	82.7	91.4	88.6

Our method offers many advantages in cost, portability, reduced set-up time, and ease of understanding without any expertise. These originate from the use of off-the-shelf, low-cost hardware. The scoring algorithm described here is the new method with PPP to score the human balance on the wobble balance board. The user can understand balance ability and the balance improvement after a balance-training cycle from this balance score. According to calculating the \max_{α} , the balance ability of the human body on the wobble balance board was affected by factors such as the height of the user (the COM position) and the foot position. Besides that, the hardware used here has certain limitations that can be listed. The balance board can only support limited weight. The limitations of RGB cameras also affect the key body points for extracting, for example, the camera's improper lighting and focal length. Objective factors such as the user's clothes and the user's position can adversely influence the measurement.

7. Conclusions

This study proposed a new algorithm to score the human body-balance ability on the wobble board (HBBAWB), based on a geometric solution using a cheap and portable device. The method utilized an equivalent model, based on visual information, expressed as an inverted pendulum on a wobble board with three joints. The location of the inverted pendulum indicated the center of mass (COM) for humans. Human movements affected the wobble slope because the wobble board was the free joint, which meant there was no

actuation. Moreover, this study defined the new index as the perpendicular-projection point (PPP), which was the projected point of the COM on the tilted plane. The proposed geometric solution utilized the relationship among the three PPP, COM, and BOF points, which meant the middle point between the two feet was via linear regression. Although it was limited by inviting only older adults to join the experiment, the results are still presented comprehensibly.

In addition, the experimental results found that the geometric solution, which utilized the relationship between the three angles of the equivalent model, enabled us to score the HBBAWB, which supports the user in understanding the balance ability and balance improvement in balance training. This research creates a premise for our following improving study in the future, with deep-learning frameworks.

Author Contributions: Conceptualization, Methodology, Writing—original draft, H.T.P.N. and H.J.; Data curation, Y.W. and N.N.H.; Formal analysis, Investigation, H.T.P.N., Y.W. and H.J.; Project administration, Supervision, H.J.; Software, H.T.P.N. and Y.W.; Visualization, H.T.P.N. and N.N.H.; Writing—review & editing, H.T. P.N., Y.W., N.N.H. and H.J. All authors have read and agreed to the published version of the manuscript.

Funding: This research was funded by the Basic Science Research Program, through the National Research Foundation (NRF) of Korea grant, funded by the Ministry of Education (No. 2021R1I1A3055210 1240982119420102) and the Korea Innovation Foundation, through the R&D innovation cluster of the Republic of Korea (No. 2022-DD-RD-0065-01-20440982119420101).

Institutional Review Board Statement: The study was conducted according to the guidelines of the Declaration of Helsinki, and approved by the Institutional Review Board (or Ethics Committee) of Applied Sciences (ISSN 2076-3417; CODEN: ASPCC7) which is an international, peer-reviewed, open access journal on all aspects of applied natural sciences published semimonthly online by MDPI.

Informed Consent Statement: After the authors explained the objectives and procedures of this study, the informed consent was obtained from all subjects. The experimental procedures were performed under the Declaration of Helsinki.

Acknowledgments: The authors would like to express a huge thank you to the BK21 Plus program at Chonnam National University, through the National Research Foundation, funded by the Ministry of Education of Korea. And the authors also would like to say thanks to participants who joined our experiments.

Conflicts of Interest: The authors declare no conflict of interest.

References

1. Hrysomallis, C. Relationship between balance ability, training and sports injury risk. *Sport Med.* **2007**, *37*, 547–556. [[CrossRef](#)]
2. McGuine, T.A.; Greene, J.J.; Best, T.; Levenson, G. Balance as a predictor of ankle injuries in high school basketball players. *Clin. J. Sport Med.* **2000**, *10*, 239–244. [[CrossRef](#)]
3. Watson, A.W. Ankle sprains in players of the field-games gaelic football and hurling. *J. Sport Med. Phys. Fit* **1999**, *39*, 66–70.
4. Goodworth, A.D.; Johnson, M.J.; Popovic, M.B. Chapter 12: Physical Therapy and Rehabilitation. In *Biomechanics*; Academic Press, Elsevier: Amsterdam, The Netherlands, 2019; pp. 333–372. [[CrossRef](#)]
5. Woo, Y.; Ko, S.; Ahn, S.; Nguyen, H.T.P.; Shin, C.; Jeong, H.; Noh, B.; Lee, M.; Park, H.; Youm, C. Classification of Diabetic Walking for Senior Citizens and Personal Home Training System Using Single RGB Camera through Machine Learning. *Appl. Sci.* **2021**, *11*, 9029. [[CrossRef](#)]
6. Woo, Y.; Andres, P.T.C.; Jeong, H.; Shin, C. Classification of diabetic walking through machine learning: Survey targeting senior citizens. In Proceedings of the 2021 International Conference on Artificial Intelligence in Information and Communication (ICAIIIC), Jeju Island, Korea, 20–23 April 2021; Jang, Y.M., Ed.; IEEE: New York, NY, USA; pp. 435–437.
7. Gebel, A.; Prieske, O.; Behm, D.G.; Granacher, U. Effects of Balance Training on Physical Fitness in Youth and Young Athletes: A Narrative Review. *Strength Cond. J.* **2020**, *42*, 35–44. [[CrossRef](#)]
8. Boccolini, G.; Brazziti, A.; Bonfanti, L.; Alberti, G. Using balance training to improve the performance of youth basketball players. *Sport Sci. Health* **2013**, *9*, 37–42. [[CrossRef](#)]
9. Anna, B.; Anna, K.; Justyna, M.; Michał, P.; Kajetan, J.S.; Grzegorz, J. Balance Training Programs in Athletes—A Systematic Review. *J. Hum. Kinetics* **2017**, *58*, 45–64.
10. Chen, H.M.; Chen, C.M. Factors Associated with Quality of Life Among Older Adults with Chronic Disease in Taiwan. *Int. J. Gerontol.* **2017**, *11*, 12–15. [[CrossRef](#)]

11. Taware, G.; Agrawal, R.; Dhende, P.; Jondhalekar, P.; Hule, S. AI-based Workout Assistant and Fitness guide. *Int. J. Eng. Res. Technol.* **2021**, *10*.
12. Mutz, M.; Müller, J.; Reimers, A.K. Use of digital media for home-based sports activities during the COVID-19 pandemic: Results from the German SPOVID survey. *Int. J. Environ. Res. Public Health* **2021**, *18*, 4409. [CrossRef]
13. Editorial. Top 8 AI-Based Personal Trainers. The Future Of Fitness. 2021. Available online: <https://roboticsbiz.com/top-8-ai-based-personal-trainers-the-future-of-fitness/> (accessed on 29 March 2022).
14. Tatariants, M. Challenges of Human Pose Estimation in AI-Powered Fitness Apps. 2020. Available online: <https://www.infoq.com/articles/human-pose-estimation-ai-powered-fitness-apps/> (accessed on 29 March 2022).
15. Ko, S.; Ahn, S.; Lee, J.; Woo, J.; Jeong, H.; Shin, C. Development of Fitness Personal Trainer with 3D Human Pose Estimation from 2D Images. In Proceedings of the 21st International Conference on Control, Automation and Systems, Ramada Plaze, Jeju Island, Korea, 12–15 October 2021.
16. Menolotto, M.; Komaris, D.S.; Tedesco, S.; O’Flynn, B.; Walsh, M. Motion capture technology in industrial applications: A systematic review. *Sensors* **2020**, *20*, 5687. [CrossRef] [PubMed]
17. Lee, C.H.; Sun, T.L. Evaluation of postural stability based on a force plate and inertial sensor during static balance measurements. *J. Physiol. Anthropol.* **2018**, *37*, 27. [CrossRef]
18. Wade, L.; Needham, L.; McGuigan, P.; Bilzon, J. Applications and limitations of current markerless motion capture methods for clinical gait biomechanics. *PeerJ* **2022**. [CrossRef]
19. Jeong, H.; Yamada, K.; Kido, M.; Okada, S.; Nomura, T.; Ohno, Y. Analysis of Difference in Center-of-Pressure Positions Between Experts and Novices During Asymmetric Lifting. *IEEE J. Trans. Eng. Health Med.* **2016**, *4*, 2100311. [CrossRef]
20. Jeong, H.; Ohno, Y. Symmetric lifting posture recognition of skilled experts with linear discriminant analysis by center-of-pressure velocity. *Intell. Serv. Robotics* **2017**, *10*, 323–332. [CrossRef]
21. Wang, T.; Jeong, H.; Watanabe, M.; Iwatani, Y.; Ohno, Y. Fault classification with discriminant analysis during sit-to-stand movement assisted by a nursing care robot. *Mech. Syst. Signal Process.* **2018**, *113*, 90–101. [CrossRef]
22. Wang, T.; Jeong, H.; Ohno, Y. Evaluation of Self-Reliance Support Robot through Relative Phase. *IEEE Access* **2017**, *5*, 17816–17823. [CrossRef]
23. MediaPipe Pose. Available online: <https://google.github.io/mediapipe/solutions/pose> (accessed on 10 October 2021).
24. Kaichi, T.; Mori, S.; Saito, H.; Takahashi, K.; Mikami, D.; Isogawa, M.; Kusachi, Y. Image-based center of mass estimation of the human body via 3D shape and kinematic structure. *Sports Eng.* **2019**, *22*, 17. [CrossRef]
25. Fang, C.C.; Hsu, C.H.; Chiu, C.W.; Kung, J.T.; Shih, H.C. Center of Mass Trajectory: An Image Descriptor For Baseball Swing Analysis Based On Single Low-Cost Camera. In Proceedings of the 2021 IEEE International Conference on Multimedia & Expo Workshops (ICMEW), Shenzhen, China, 5–9 July 2021; IEEE: New York, NY, USA; Volume 1, pp. 1–5.
26. De Leva, P. Adjustments to Zatsiorsky-Seluyanov’s segment inertia parameters. *J. Biomech.* **1996**, *29*, 1223–1230. [CrossRef]
27. Aftab, Z.; Robert, T.; Wieber, P.B. Balance Recovery Prediction with Multiple Strategies for Standing Humans. *PLoS ONE* **2016**, *11*, e0151166. [CrossRef]
28. Waldron, K.J.; Schmiedeler, J. Chapter 1: Kinematics. In *Springer Handbook of Robotics*; Springer: Berlin/Heidelberg, Germany, 2016. [CrossRef]
29. Takeda, K.; Mani, H.; Hasegawa, N.; Sato, Y.; Tanaka, S.; Maejima, H.; Asaka, T. Adaptation effects in static postural control by providing simultaneous visual feedback of center of pressure and center of gravity. *J. Physiol. Anthropol.* **2017**, *36*, 31. [CrossRef] [PubMed]
30. Winter, D.A. Human balance and posture control during standing and walking. *Gait Posture* **1995**, *3*, 193–214. [CrossRef]
31. Newell, A.; Yang, K.; Deng, J. Stacked hourglass networks for human pose estimation. In Proceedings of the European Conference on Computer Vision, Amsterdam, The Netherlands, 11–14 October 2016.
32. Sigal, L.; Balan, A.O.; Black, M.J. HumanEva: Synchronized video and motion capture dataset and baseline algorithm for evaluation of articulated human motion. *Int. J. Comput. Vis.* **2010**, *8*, 4–27. [CrossRef]
33. Ionescu, C.; Papava, D.; Olaru, V.; Sminchisescu, C. Human3.6M: Large scale datasets and predictive methods for 3D human sensing in natural environments. *IEEE Trans. Pattern Anal. Mach. Intell.* **2014**, *36*, 1325–1339. [CrossRef] [PubMed]
34. Desmarais, Y.; Mottet, D.; Slangen, P.; Montesinos, P. A review of 3D human pose estimation algorithms for markerless motion capture. *Comput. Vis. Image Underst.* **2021**, *212*, 103275. [CrossRef]
35. Intel Corporation, Willow Garage, Itseez, OpenCV. Available online: <https://opencv.org/> (accessed on 30 March 2022).
36. Cao, Z.; Simon, T.; Wei, S.E.; Sheikh, Y. OpenPose: Realtime Multi-Person 2D Pose Estimation using Part Affinity Fields. *IEEE Trans. Pattern Anal. Mach. Intell.* **2021**, *43*, 172–186. [CrossRef]
37. Kendall, A.; Grimes, M.; Cipolla, R. PoseNet: A Convolutional Network for Real-Time 6-DOF Camera Relocalization. In Proceedings of the IEEE International Conference on Computer Vision (ICCV), Santiago, Chile, 11–18 December 2015; pp. 2380–7504.
38. Wu, Y.; Kirillov, A.; Massa, F.; Lo, W.; Girshick, R. Detectron2. Available online: <https://detectron2.readthedocs.io/en/latest/> (accessed on 30 March 2022).
39. Fang, H.S.; Xie, S.; Tai, Y.W.; Lu, C. RMPE: Regional multi-person pose estimation. In Proceedings of the IEEE International Conference on Computer Vision (ICCV), Venice, Italy, 22–29 October 2017; pp. 2353–2362.

40. Bazarevsky, V.; Grishchenko, I.; Raveendran, K.; Zhu, T.; Zhang, F.; Grundmann, M. BlazePose: On-device Real-time Body Pose tracking. In Proceedings of the CVPR Workshop on Computer Vision for Augmented and Virtual Reality, Online, 17 June 2020.
41. Xu, H.; Bazavan, E.G.; Zafir, A.; Freeman, W.T.; Sukthankar, R.; Sminchisescu, C. Ghum & ghuml: Generative 3d human shape and articulated pose models. In Proceedings of the IEEE/CVF Conference on Computer Vision and Pattern Recognition(CVPR), Seattle, WA, USA, 16–18 June 2020; pp. 6184–6193.